

Published in final edited form as:

*Blood*. 2009 July 9; 114(2): 318–327. doi:10.1182/blood-2008-10-184457.

## Differential signal transduction, membrane trafficking, and immune effector functions mediated by Fc $\gamma$ RI versus Fc $\gamma$ RIIa

Xilei Dai<sup>1</sup>, Manikandan Jayapal<sup>2</sup>, Hwee Kee Tay<sup>2</sup>, Renji Reghunathan<sup>2</sup>, Gen Lin<sup>1</sup>, Chien Tei Too<sup>1</sup>, Yan Ting Lim<sup>1</sup>, Soh Ha Chan<sup>1</sup>, D. Michael Kemeny<sup>1</sup>, R. Andres Floto<sup>3</sup>, Kenneth G. C. Smith<sup>3</sup>, Alirio J. Melendez<sup>2,4</sup>, and Paul A. MacAry<sup>1</sup>

<sup>1</sup>Departments of Microbiology, National University of Singapore, Singapore

<sup>2</sup>Departments of Physiology, National University of Singapore, Singapore

<sup>3</sup>Department of Medicine/CIMR University of Cambridge, Cambridge, United Kingdom;

<sup>4</sup>Division of Immunology, Infection and Inflammation, University of Glasgow, Glasgow, United Kingdom

### Abstract

Receptors for the fragment crystallizable region of immunoglobulin-G (Fc $\gamma$ RS) play an important role in linking the humoral and cellular arms of the immune response. In this study, we present a comprehensive functional comparison of 2 human Fc-receptors, Fc $\gamma$ RI and Fc $\gamma$ RIIa. Activation of Fc $\gamma$ RI results in a novel signaling cascade that links phospholipase D1 to sphingosine kinase-1 in U937 cells and primary human monocytes. This induces the expression of proinflammatory mediators and is associated with trafficking of immune complexes into human leukocyte antigen-DM positive antigen-processing compartments coupled with improved MHC class II-mediated antigen presentation to T lymphocytes. In contrast, activation of Fc $\gamma$ RIIa elicits signaling through phospholipase C $\gamma$ 1, resulting in increases in intracellular calcium, activation of nicotinamide adenine dinucleotide phosphate oxidative burst, and differential membrane trafficking combined with impaired antigen presentation and proinflammatory cytokine expression. These data provide a mechanistic insight into the disparate activities associated with Fc receptors in immunity, namely, reinforcement of immune responses through stimulation of proinflammatory signaling and antigen presentation, versus the maintenance of immunologic homeostasis through the noninflammatory clearance of immune complexes.

---

Correspondence: Paul A. MacAry, Immunology Program, Department of Microbiology, Center for Life Sciences, Singapore 129793; micpam@nus.edu.sg. Alirio J. Melendez, Division of Immunology, Infection and Inflammation, Glasgow Biomedical Research Center, University of Glasgow, Glasgow G12 8TA, United Kingdom; a.melendez-romero@clinmed.gla.ac.uk.

#### Authorship

Contribution: X.D., M.J., H.K.T., R.R., G.L., C.T.T., and Y.T.L. performed experiments; X.D., M.J., and H.K.T. analyzed results; X.D., M.J., and H.K.T. made the figures; R.A.F., K.G.C.S., S.H.C., and D.M.K. provided reagents and support for the research; and X.D., A.J.M., and P.A.M. designed the research and wrote the paper.

Conflict-of-interest disclosure: The authors declare no competing financial interests.

## Introduction

Fragment crystallizable receptors (FcRs) are receptors on immune cells that bind to the Fc region of immunoglobulins. Fc $\gamma$ Rs that bind to the most common type of immunoglobulin (IgG), are expressed on the surface of many different immune cell types including monocytes, macrophages, dendritic cells, and neutrophils.<sup>1–3</sup> In humans, 3 different classes of activatory IgG receptors have been defined: Fc $\gamma$ RI (CD64), Fc $\gamma$ RIIa (CD32a), and Fc $\gamma$ RIII (CD16), each of which has a variety of isoforms with differing affinities for IgG, tissue distribution, and level of expression.<sup>1–6</sup> The high affinity IgG receptor, Fc $\gamma$ RI, is a 72-kD type-I membrane glycoprotein constitutively expressed on monocyte and macrophage lineage cells.<sup>4</sup> Fc $\gamma$ RI is a member of the multichain immune recognition receptor family, comprising hetero-oligomeric complexes of a ligand-binding  $\alpha$ -chain and a signaling  $\gamma$ -chain usually found in association with other immune receptors.<sup>1–6</sup> The  $\gamma$ -chain contains a signaling motif termed the “immunoreceptor tyrosine-based activation motif” (ITAM): it is through the ITAM-bearing chain that most FcRs trigger intracellular signal transduction cascades. The low-affinity receptor, Fc $\gamma$ RIIa, is the most broadly distributed human Fc $\gamma$ R and is expressed on many cell types, such as monocytes, neutrophils, and platelets.<sup>1,7</sup> This low-affinity receptor preferentially binds complexes of IgG and is the only Fc receptor that contains an ITAM of its own. Thus, it is the only Fc receptor that does not need to oligomerize with a  $\gamma$ -chain in order to signal.<sup>4,8,9</sup> There is no identified murine equivalent of Fc $\gamma$ RIIa.<sup>1</sup>

On myeloid cells, aggregation of Fc $\gamma$ Rs during the early stages of infection leads to several cellular responses, including the internalization of immune complexes by endocytosis or opsonized particles through phagocytosis, degranulation with the release of proteases, activation of respiratory burst, and secretion of cytokines.<sup>5,10–12</sup> The presentation of antigens derived from internalized complexes forms an important component of our adaptive immune response, and dysregulation of this pathway is reported to be linked to increased susceptibility to bacterial sepsis.<sup>13</sup> The safe clearance of immune complexes toward the latter stages of infection is also dependent on FcR expressing mononuclear phagocytes. Dysfunction in the clearance of immune complexes is reported to be associated with immunopathology, autoimmunity, and allergic disease.<sup>9,14</sup> This represents one of the critical but poorly understood functions of Fc receptors, ie, the determination of the antigenic fate of immune complexes; specifically, whether to internalize and digest them in a way that is noninflammatory or to reinforce antigen presentation combined with immune activation and associated proinflammatory signaling.

Studies on differential functions mediated by individual Fc receptors in immune activation/homeostasis are complicated by the coexistence of several FcRs on phagocytic cells—it is difficult to identify the signaling cascades and functions triggered by one specific receptor, when they are cross-linked by a multivalent ligand (ie, IgG complexes). Nevertheless, it has been shown that aggregation of Fc $\gamma$ RI or Fc $\gamma$ RIIa results in signal transduction events evidenced by tyrosine phosphorylation of proteins,<sup>2,12</sup> calcium release from internal stores,<sup>8,15,16</sup> and the activation of various phospholipases and lipid kinases.<sup>8,10,12,16–19</sup> It has been intimated that Fc $\gamma$ RI is constitutively associated with detergent-insoluble lipid microdomains in the absence of ligand cross-linking<sup>20</sup> and that Fc $\gamma$ RI<sup>-/-</sup> mice exhibit

impaired antigen presentation and cytokine production.<sup>21</sup> In contrast, Fc $\gamma$ RII requires ligand cross-linking for association with lipid rafts.<sup>22</sup> In this study, we compare and contrast the signaling pathways elicited by human Fc $\gamma$ RI and Fc $\gamma$ RIIa in U937 and primary human monocytes and address the role of these receptors in membrane trafficking and presentation of influenza A virus antigens delivered as part of human IgG immune complexes.

## Methods

All the chemicals and reagents are of molecular biology grade and from Sigma-Aldrich unless otherwise specified. This research was conducted under a protocol approved by the National University of Singapore Institutional Review Board covering all work described with human blood-derived cells and antibodies. All blood was collected after informed consent was obtained in accordance with the Declaration of Helsinki.

### Tissue culture and Fc $\gamma$ RI and Fc $\gamma$ RIIa receptor aggregation

The human monocytic cell line U937 (ATCC) was grown in normal growth medium and treated with 100-ng/mL IFN- $\gamma$  (PeproTech) overnight.<sup>23</sup> The next day, the cells were washed and divided into 2 and treated with 1  $\mu$ M of mouse anti-human CD64 and mouse anti-human CD32 antibodies (Murine IgG1 clones 10.1 and 3D3, respectively, BD Pharmingen) for 45 minutes at 4°C, with tumbling to occupy surface Fc $\gamma$ Rs. Murine IgG1 antibodies were used to ensure minimal cross-reactivity with human FcRs.<sup>24</sup> Excess unbound ligand was removed by serial washing in medium. Cells were resuspended in ice-cold medium, and surface immune complexes were formed by incubating with cross-linking antibodies (goat anti-mouse IgG F(ab')<sub>2</sub> 1:50) for 10 minutes at 4°C. Cells were washed 2 times to remove unbound goat IgGs. Cells were then incubated at 37°C for the times stated in the Results section.

### Preparation of primary human monocytes

Primary human monocytes were prepared from fresh human blood samples taken under informed consent from volunteer human donors. Monocytes in unfractionated peripheral blood exhibited significant surface staining with goat anti-mouse F(ab')<sub>2</sub> (Thermo Scientific), suggesting a significant degree of FcR occupancy by monomeric IgGs (see supplemental Figure 1Ai, available on the *Blood* website; see the Supplemental Materials link at the top of the online article). Purified monocytes were isolated using anti-CD14 microbeads (Miltenyi Biotec) and washed 8 times in 100 $\times$ volumes of ice-cold citrate buffer (PBS/0.4% sodium citrate) before culture and use in serum-free medium (AIM V or DMEM, Invitrogen). Monocytes prepared in this way exhibit a significant reduction in surface staining for human IgG (see supplemental Figure 1Aii) and show significant binding activity for exogenous human IgG (see supplemental Figure 1Aiii). All monocytes used in this study were selected based on negligible surface staining for CD16 by flow cytometry (see supplemental Figure 2C).

### Intracellular signaling assays in U937 and primary human monocytes

Cytosolic Ca<sup>2+</sup> measurement; phospholipase C and phospholipase D activity, chemical inhibition experiments, fluorescent microscopy, and protein kinase C (PKC) enzyme activity

assay; subcellular fractionation; and Western blots were performed as described previously. 8,10,16–18,25–28 Antisense knockdown, antisense oligonucleotides were from 1st Base for PLD1, 5'-CCGTGGCTCGTTTTTCAGTG-3'; PLD1-scrambled control, 5'-TTCCTTGGGTTCCGCTTGGGA-3'; PLC $\gamma$ 1, 5-GGGGACGCGGCGCCCGCCAT-3; and PLC $\gamma$ 1-scrambled control, 5-CTGGTGGGAAGAAGAGGACGT-3. Transfections were performed as previously described.<sup>27–29</sup> Phosphoprotein arrays, 8-plex phosphoprotein arrays (Bio-Rad) were used to assay cell lysates for phosphorylation of Akt, MEK, ERK1 or ERK2, p38, Jnk, NF $\kappa$ B, c-Jun, and Src. The assay was conducted per the manufacturer's instructions.

### Effector response assays

For the nicotinamide adenine dinucleotide phosphate (NADPH)–oxidase assay, superoxide production was measured using an enhanced luminol-based substrate (National Diagnostics), as previously described.<sup>25</sup> For the degranulation assay, degranulation was measured using a colorimetric assay to assess the release of  $\beta$ -hexosaminidase as previously described.<sup>27,28</sup> For quantitative RT-PCR, quantitative PCR was performed as previously described.<sup>30,31</sup> For amplicon detection, the LightCycler RNA Master SYBR Green Kit (Roche) was used as described by the manufacturer, and the PCR was performed in a LightCycler instrument (Roche). For the cytokine array, a 17-plex cytokine array (Bio-Rad) was used to assay the supernatants for the following targets: IL-1 $\beta$ , IL-2, IL-4, IL-5, IL-6, IL-7, IL-8, IL-10, IL-12p70, IL-13, IL-17, GM-CSF, IFN- $\gamma$ , TNF- $\alpha$ , G-CSF, MCP-1, and MIP-1 $\beta$ . The assay was conducted per the manufacturer's instructions.

### Stimulation of primary monocytes with immune complexes

The generation of human IgG/influenza A immune complexes is detailed in the supplementary Methods section. Monocytes were resuspended in 200  $\mu$ L of serum-free AIM-V media (Invitrogen). To block Fc $\gamma$ RI, 10  $\mu$ M of human IgG (Sigma-Aldrich) was added to the cells. We confirmed that at this concentration, the immune complexes (IC) used for 10 minutes at a titration of 1:5 do not exhibit significant surface binding to Fc $\gamma$ RI through displacement of surface monomeric IgG (see supplemental Figure 1B). To block Fc $\gamma$ R2, 100  $\mu$ g/mL of IV.3 monoclonal antibody was added to the cells (ATCC).<sup>32</sup> The cells were incubated with these blocking antibodies for 1 hour at 4°C. They were then washed with PBS and resuspended in 200  $\mu$ L of AIM-V media each; 25  $\mu$ L of immune complex was then added to each sample and incubated at 37°C for 10 minutes to induce immune complex internalization or cellular signaling.

### T-cell proliferation assay

The generation of influenza-specific CD4<sup>+</sup> T cells is detailed in the supplementary Materials section.  $\alpha$ -PR8 CD4<sup>+</sup> T cells were plated in a 96-well plate (100  $\mu$ L of  $2 \times 10^6$  cells/mL);  $4 \times 10^4$  treated CD14<sup>+</sup> were treated in the following way: (1) untreated, (2) Fc $\gamma$ RI-induced immune complex uptake for 10 minutes, (3) Fc $\gamma$ R2-induced immune complex uptake for 10 minutes, and (4) immune complex uptake for 10 minutes through both Fc $\gamma$ RI and Fc $\gamma$ R2. Aliquots of (1)-(4) were then added to the plate. The APC to T-cell ratio used was 1:5, and they were incubated at 37°C and 5% CO<sub>2</sub> for 4 to 7 days, until the T cells could be seen to

be proliferating. Cell proliferation was measured by the  $^3\text{H}$ -thymidine method as previously described.<sup>33</sup>

### IFN- $\gamma$ ELISPOT

The assay was carried out as previously described.<sup>34</sup> Briefly, freshly isolated human peripheral mononuclear cells, washed 8 times in 100 $\times$  volumes of ice-cold citrate buffer and depleted of CD8 $^+$  were treated with immune complexes as described above in steps 1 through 4 in “T-cell proliferation assay” and resuspended in AIM-V media (Invitrogen) with 2% human AB serum at a concentration of  $2 \times 10^6$  cells/mL, then the cells were plated (100 $\mu\text{L}$  cells/well) into a 96-well plate. The plate was incubated at 37°C for 16-18 hours, washed, and 100  $\mu\text{L}$  of 0.5  $\mu\text{g}/\text{mL}$  biotinylated 7-B6-1 was added to each well and incubated for 2 hours; 100  $\mu\text{L}$  of 1:2000 dilution of streptavidin-ALP was then added to each well and incubated for 1 hour; 50  $\mu\text{L}$  of the BCIP/NBT substrate was then added to each well for 2 minutes. After a final wash the plate was left to dry and read using the CTL ImmunoSpot S4 Analyzer (Cellular Technology Ltd).

### Statistical analysis

Results for the phosphoprotein array, IFN- $\gamma$  ELISPOT, and the proliferation assay were first analyzed using analysis of variance (ANOVA). Upon obtaining a significant  $F$  value, a Tukey protected  $t$  test was then conducted, comparing the results obtained by stimulating the cells with either Fc $\gamma$ RI and/or Fc $\gamma$ RII cross-linking.

## Results

### Monocyte-differentiated U937 cells express Fc $\gamma$ RI and Fc $\gamma$ RIIa but not Fc $\gamma$ RIIb1/2

U937 is a premonocytic cell line that expresses high levels of surface Fc $\gamma$ RIIa and low levels of surface Fc $\gamma$ RI. When U937 cells are treated with IFN- $\gamma$ , the expression of Fc $\gamma$ RI detected on the cell surface by flow cytometry increases. U937 cells do not express Fc $\gamma$ RIII under these culture conditions (Figure 1A). We performed RT-PCR analyses to test for expression of the immune-tyrosine inhibitory motif-containing inhibitory FcR, Fc $\gamma$ RIIb1/2. Primers specific for Fc $\gamma$ RIIb1/2 were used to detect the expression of this receptor in human B cells and dendritic cells.<sup>35</sup> Fc $\gamma$ RIIb1/2 transcripts were undetectable in U937 (Figure 1B).

### Differential calcium signaling induced by Fc $\gamma$ RI versus Fc $\gamma$ RIIa

It has previously been shown that cross-linking Fc $\gamma$ RI and Fc $\gamma$ RII on U937 results in increases in intracellular calcium.<sup>15</sup> We have previously extended these studies to show that in IFN- $\gamma$ -treated U937, Fc $\gamma$ RI induces coupling of phospholipase D with sphingosine kinase to trigger a single “spike” of calcium of relatively short duration, released from internal stores.<sup>16</sup> Here, we examined whether the same mechanism is used by the low-affinity IgG receptor (Fc $\gamma$ RIIa). In contrast to Fc $\gamma$ RI, Fc $\gamma$ RIIa triggers a calcium response for a longer duration (Figure 1C). Whereas Fc $\gamma$ RI elicits a short-lived calcium response that lasts for 2 minutes, Fc $\gamma$ RIIa triggers a response that lasts for more than 1 minute (Figure 1C). We next determined whether Fc $\gamma$ RIIa is linked to the same lipid signaling pathways used by Fc $\gamma$ RI. We investigated coupling of Fc $\gamma$ RIIa to the PLD-SPHK pathway. As expected, Fc $\gamma$ RI aggregation triggers PLD activity (Figure 1D). In contrast, Fc $\gamma$ RIIa did not

trigger a significant rise in PLD activation (Figure 1D). As no PLD activation was triggered by Fc $\gamma$ RIIa aggregation, we determined whether the phospholipase C pathway triggers the observed calcium signals. Aggregation of Fc $\gamma$ RIIa elicits a significant transient rise in InsP<sub>3</sub> levels in U937 (Figure 1E). In contrast, no InsP<sub>3</sub> could be detected after Fc $\gamma$ RI aggregation (Figure 1E). Furthermore, an inhibitor of PLC, U73122, that blocks the calcium response triggered by Fc $\gamma$ RIIa had no effect on Fc $\gamma$ RI (Figure 1F). This confirms that the 2 receptors couple to different phospholipid signaling molecules to trigger intracellular calcium signals. Phosphoprotein array results also indicate that cross-linking Fc $\gamma$ RI activates the MEK1/ERK pathway to a greater extent, compared with Fc $\gamma$ RIIa in IFN- $\gamma$ -treated U937. These observations can also be extended to primary human monocytes in which cross-linking Fc $\gamma$ RI results in a significantly stronger induction of both phospho-MEK1 and phospho-ERK1/2 compared with Fc $\gamma$ RIIa (Figure 1G).

### Fc $\gamma$ RIIa triggers the activation of PLC $\gamma$ 1

We investigated which isoform of PLC is involved in Fc $\gamma$ RIIa signaling by immunoblot and fluorescence microscopy on cellular fractions. After Fc $\gamma$ RIIa aggregation, PLC $\gamma$ 1 rapidly translocates to the nuclear-free membrane fraction, whereas no PLC $\gamma$ 1 could be detected in the membrane fraction prepared from resting cells (Figure 2A). Thus, 30 seconds after Fc $\gamma$ RIIa aggregation, a band corresponding to the correct molecular weight for PLC $\gamma$ 1 was detected in the membrane fraction and remained associated with this fraction up to 5 minutes (30 seconds, 1 minute, 2 minutes, and 5 minutes; Figure 2A). These results were confirmed by fluorescence microscopy—in resting cells, PLC $\gamma$ 1 has a homogenous cytosolic distribution before Fc $\gamma$ RIIa aggregation. After Fc $\gamma$ RIIa aggregation, PLC $\gamma$ 1 redistributes to the cell periphery, exhibiting a plasma membrane localization (Figure 2B). Using antisense oligonucleotides specific for PLC $\gamma$ 1, we knocked down PLC $\gamma$ 1 expression levels (Figure 2C). When InsP<sub>3</sub> and calcium responses were triggered by Fc $\gamma$ RIIa, we observed that both signals were substantially reduced (Figure 2D and E, respectively), whereas Fc $\gamma$ RI aggregation retained its ability to stimulate calcium responses (Figure 2E).

### Fc $\gamma$ RI and Fc $\gamma$ RIIa activate different PKC isoforms

We have previously shown that Fc $\gamma$ RI triggers a fast activation of PKC activity.<sup>18</sup> When we compare the kinetics of PKC activation, we observed that Fc $\gamma$ RI triggers an initial rise in PKC activity, followed by a sustained increase over a 45-minute period (Figure 2F). In contrast, Fc $\gamma$ RIIa aggregation triggers a more rapid PKC response, reaching a plateau at 3 minutes, which is maintained over the 45-minute time course (Figure 2F).

Intracellular calcium has been proposed to be an important cofactor for PKC activity. However, we have previously shown that Fc $\gamma$ RI triggers calcium-independent PKC activity.<sup>18</sup> It has been shown that the amplitude and modulation of a calcium response can influence PKC isoform activation, so we investigated the calcium dependence of Fc $\gamma$ RIIa-triggered PKC activation. As previously reported,<sup>18</sup> the increase in PKC activity after Fc $\gamma$ RI aggregation was unaffected by the withdrawal of calcium from the assay (Figure 2G). In contrast, withdrawal of calcium completely abolished any increase in PKC activity after Fc $\gamma$ RIIa aggregation (Figure 2G). These results demonstrate that Fc $\gamma$ RIIa triggers the activation of calcium-dependent PKC isoforms.

As PKC activation is associated with translocation to plasma membranes, we investigated whether Fc $\gamma$ RI and Fc $\gamma$ RIIa result in differential activation of particular PKC isoforms. Using subcellular fractionation, we show that Fc $\gamma$ RI triggers the translocation of the calcium-independent PKCs  $\delta$ ,  $\epsilon$ , and  $\zeta$  isoforms from the cytosol to the plasma membrane (Figure 2H). In contrast, Fc $\gamma$ RIIa aggregation induces the translocation of the calcium-dependent PKC  $\alpha$ ,  $\beta$ , and  $\gamma$  isoforms (Figure 2I). Taken together, these results show that there is a marked difference in the specific PKC isoforms activated by Fc $\gamma$ RI versus Fc $\gamma$ RIIa.

### **Fc $\gamma$ RI-triggered PKC activity and isoform translocation are dependent on PLD1; Fc $\gamma$ RIIa-triggered PKC activity and isoform translocation are dependent on PLC $\gamma$ 1**

In cells pretreated with an antisense specific for PLD1, cross-linked Fc $\gamma$ RI-triggered PKC activity and isoform translocation were substantially inhibited. No inhibition was observed in parallel U937 cells treated with antisense PLC $\gamma$ 1 (Figure 3A and B, respectively). When we cross-linked Fc $\gamma$ RIIa in cells where PLC $\gamma$ 1 was knocked down, PKC enzyme activity and PKC isoform translocation were substantially reduced. No inhibition was observed in cells where PLD1 had been knocked down (Figure 3A and C, respectively).

### **Different signaling molecules are involved in Fc $\gamma$ RI and Fc $\gamma$ RIIa induced degranulation and oxidative burst**

Intracellular calcium and PKC activity are linked to the release of granular contents (degranulation) and also to the NADPH-oxidative burst in U937.36,37 We investigated whether Fc $\gamma$ RI and Fc $\gamma$ RIIa cross-linking results in differences in these responses. In contrast to the differences observed in calcium signals and PKC activation, broadly similar levels of  $\beta$ -hexosaminidase release (degranulation) were triggered by Fc $\gamma$ RI and Fc $\gamma$ RIIa (Figure 3Di and ii). We also observed that Fc $\gamma$ RI-triggered  $\beta$ -hexosaminidase release is dependent on PLD1 and not PLC $\gamma$ 1 (Figure 3Di). In contrast, Fc $\gamma$ RIIa-triggered  $\beta$ -hexosaminidase release was dependent on PLC $\gamma$ 1 and not PLD1 (Figure 3Dii). Moreover, the activation of the NADPH-oxidative burst exhibited different kinetics between the 2 receptors (Figure 3Ei and ii). Fc $\gamma$ RI-triggered NADPH-activity depends on PLD1 (Figure 3Ei), whereas the Fc $\gamma$ RIIa-triggered oxidative burst depends on PLC $\gamma$ 1 (Figure 3Eii). These results suggest that although the cellular functions of degranulation and oxidative burst are triggered by either receptor, the nature and kinetic of the signals that induce these functional responses are different.

We tested whether the link between Fc $\gamma$ RI and PLD1 and PLC $\gamma$ 1 and Fc $\gamma$ RIIa signaling in U937 could also be extended to primary human monocytes. In primary monocytes treated with antisense specific for PLD1 or antisense PLC $\gamma$ 1, a significant reduction in PLD1/PLC $\gamma$ 1 expression levels was observed (Figure 3Fi). In monocytes treated with antisense PLD1, a significant reduction in induced cytosolic calcium was observed after antibody-mediated aggregation of Fc $\gamma$ RI. In contrast, when Fc $\gamma$ RIIa was activated, the cytosolic calcium response was inhibited in cells treated with antisense PLC $\gamma$ 1. As with earlier observations on MEK1 and ERK1/2, these data suggest that the signaling activity associated with Fc $\gamma$ RI and Fc $\gamma$ RIIa in IFN- $\gamma$ -treated U937 can be extended to primary human monocytes (Figure 3Fii and iii).

### **Fc $\gamma$ RI and Fc $\gamma$ RIIA triggered secretion of cytokines and chemokines**

U937 cells were stimulated by cross-linking either Fc $\gamma$ RI and/or Fc $\gamma$ RIIA for 10 minutes and culture supernatants harvested 24 hours later. Supernatants were assayed for cytokine secretion with a Bio-Rad 17-plex cytokine array, and we observed that the proinflammatory cytokines and chemokines IL-8, TNF- $\alpha$ , MIP-1 $\beta$ , IL-6, and G-CSF were differentially expressed/secreted between the 2 cross-linked Fc receptors in 4 independent experiments, with triggering of Fc $\gamma$ RI inducing higher levels of secretion. (Figure 4A-F).

### **Differential membrane trafficking of Fc $\gamma$ RI and Fc $\gamma$ RIIA receptors**

In the absence of multivalent ligand, Fc $\gamma$ RI, and Fc $\gamma$ RIIA are found on the cell surface of U937 and primary monocytes (Figure 5A). Antibody-mediated aggregation induces Fc $\gamma$ RI and Fc $\gamma$ RIIA molecules to enter intracellular compartments expressing the early endosomal marker EEA-1 (Figure 5Bi) and the SNARE proteins Syntaxin 4 and TI-VAMP (see supplemental Figure 2Ai-ii). The Fc $\gamma$ RI-containing endosome exhibits positive staining for human leukocyte antigen (HLA)-DM. HLA-DM is a putative marker for MHC class II molecules are loaded with peptides derived from endocytosed antigens.<sup>38,39</sup> In contrast, cross-linked Fc $\gamma$ RIIA internalizes into compartments that show little or no costaining for HLA-DM over an identical period (Figure 5Bii). The endosomal compartment containing the Fc $\gamma$ RI receptor also exhibits a significant degree of staining for the late endosomal/lysosomal marker LAMP-1. Fc $\gamma$ RIIA positive compartments exhibited little or no colocalization with this marker over an identical period (Figure 5Biii).

We determined whether the membrane trafficking events observed in U937 are also found in primary FcR-expressing dendritic cells and monocytes. As in U937, when Fc $\gamma$ RI is cross-linked, it enters a compartment that stains for both the early endosomal marker EEA-1 (see supplemental Figure 2Bi and ii, respectively) and late endosome/lysosome marker LAMP-1 (see supplemental Figure 2Biii and iv, respectively). Fc $\gamma$ RIIA enters a compartment that costains for the early endosome marker EEA-1 (see supplemental Figure 2Bi and ii, respectively) but not LAMP-1 (see supplemental Figure 2Biii and iv, respectively).

### **Antigen presentation of Fc $\gamma$ RI and Fc $\gamma$ RIIA internalized immune complexes**

We sought to determine whether differences in signaling and intracellular trafficking mediated by Fc $\gamma$ RI and Fc $\gamma$ RIIA impacts upon antigen presentation. Influenza A virus was used as a source of antigens for these experiments. This is an orthomyxovirus that encodes several well-characterized antigenic determinants.<sup>40,41</sup> To generate human IgG against the influenza A virus, healthy human volunteers were vaccinated with the current seasonal influenza vaccine and then bled 21 to 60 days postinoculation. IgG was purified from serum samples by fast performance liquid chromatography. Hemagglutination inhibition was used to screen the purified human IgGs for binding activity to influenza A/PR/8/34 (Figure 6A). In addition, we screened the neutralizing activities of purified hIgG to influenza A/PR/8/34, by incubating live influenza A virus with the lipophilic dye 1,1'-dioctadecyl-3,3',3'-tetramethylindodi-carbocyanine (DiD),<sup>42</sup> then demonstrating a reduction in labeled virus binding to U937 mediated by hIgG (Figure 6B). Human IgG fractions with clear binding activity were used in conjunction with influenza A/PR/8/34 to construct in vitro immune

complexes, enriched and purified using a Vivaspin micro-concentrator system. Purified IC containing protein bands derived from hIgGs and virus were visualized on Coomassie-stained SDS-PAGE gels (Figure 6C).

Purified IC were used to stimulate cytosolic calcium responses via Fc $\gamma$ RI in monocytes treated with the Fc $\gamma$ RIIa-blocking antibody, IV.3, or via Fc $\gamma$ RIIa in monocytes treated with monomeric hIgGs (to block Fc $\gamma$ RI). The form and duration of the calcium responses engendered were similar to those observed using antibody cross-linking in U937 and primary monocytes (Figure 6Di). Pretreatment of the primary monocytes with the PLC inhibitor U73122 blocked IC-induced responses via Fc $\gamma$ RIIa, and the PLD inhibitor butan-1-ol blocked IC induced responses via Fc $\gamma$ RI. These data suggest that the signaling pathways identified by antibody-cross-linking specific FcRs apply when physiologic stimuli such as human IC are used (Figure 6Dii-iii). Primary human monocytes that do not express Fc $\gamma$ RIII were selected for these studies (see supplemental Figure 3C).

We addressed whether immune complexes delivered Fc $\gamma$ RI versus Fc $\gamma$ RIIa traffic to the same intracellular compartments as those observed with antibody-mediated receptor aggregation. Stained influenza antigens can be detected in HLA-DM<sup>+</sup> MIIC compartments when the complexes are internalized via Fc $\gamma$ RI in monocytes (IV.3 treated), whereas little or no colocalization is detected when the complexes are internalized via Fc $\gamma$ RIIa (monomeric IgG treated; Figure 6E).

Five influenza-specific CD4<sup>+</sup> T-lymphocyte cell lines were used to address the natural presentation of influenza antigens by proliferation assay. Influenza-specific CD4<sup>+</sup> T cells were stimulated by syngeneic monocytes pulsed with immune complexes through Fc $\gamma$ RI (IV.3 treated) or through Fc $\gamma$ RIIa (monomeric IgG treated). With 4 of 5 of these influenza-specific cell lines, immune complexes internalized via Fc $\gamma$ RI stimulated significantly higher levels of proliferation than those internalized through Fc $\gamma$ RIIa (see supplemental Figure 3A). When these data are combined, we see a small but significant increase in the influenza-specific T-cell proliferation index as determined by ANOVA analysis combined with a Tukey protected *t* test ( $P < .05$ ; Figure 6E).

ELISPOT analysis of CD4<sup>+</sup> T-cell responses in primary human blood samples further confirm the dominance of Fc $\gamma$ RI-mediated antigen presentation versus Fc $\gamma$ RIIa, with 7 of 9 donors showing a significant enhancement via Fc $\gamma$ RI and 2 of 9 showing either no preference or a small enhancement via Fc $\gamma$ RIIa (see supplemental Figure 3B). When these data are combined and fold-differences in ELISPOT numbers are compared, a significant increase is observed when IC are internalized via Fc $\gamma$ RI ( $P < .05$ ; Figure 6F). These data suggest that MHC class II presentation of influenza epitopes is more effective when immune complexes enter antigen-presenting cells through Fc $\gamma$ RI versus Fc $\gamma$ RIIa.

Taken together, our results suggest fundamental differences in the molecular mechanisms used by Fc $\gamma$ RI and Fc $\gamma$ RIIa in monocytic cells that couple distinct signaling pathways to functional differences in their cell biology and immunology.

## Discussion

The data presented in this paper demonstrate fundamental differences in intracellular signaling pathways, receptor trafficking, and antigen processing/presentation activities stimulated by the high-affinity activatory receptor for IgG (Fc $\gamma$ RI) versus the low-affinity activatory receptor for IgG (Fc $\gamma$ RIIa). Thus, in the IFN- $\gamma$ -treated monocytic cell line U937, Fc $\gamma$ RI couples to phospholipase D1 and sphingosine kinase 1 to trigger calcium release from internal stores. In contrast, aggregation of Fc $\gamma$ RIIa leads to the activation of phospholipase C $\gamma$ 1 to elicit calcium release. Moreover, we show that the PKC enzyme activity and isoform translocation induced by Fc $\gamma$ RI is dependent on phospholipase D1, whereas responses triggered by Fc $\gamma$ RIIa depend on the presence of phospholipase C $\gamma$ 1. Similarly, degranulation mediated by Fc $\gamma$ RI was dependent on PLD1, whereas the degranulation elicited through Fc $\gamma$ RIIa was dependent on PLC $\gamma$ 1. There was no observed overlap in the utilization of the different phospholipases by either receptor.

The finding that Fc $\gamma$ RI and Fc $\gamma$ RIIa activate different intracellular signaling molecules to trigger calcium signals and other responses may have profound implications for their functional activities. It is likely that Fc $\gamma$ RIIa produces a prolonged response to immune complex activation by using InsP<sub>3</sub> and inducing calcium entry to allow store refilling, thereby maintaining the calcium signal. This switch in phospholipase activation and calcium signaling results in the differential activation of protein kinase C isoforms, which are involved in several myeloid functions, including phagocytosis.<sup>43–46</sup> Differential protein kinase C signaling may explain the observation that Fc $\gamma$ RI-triggered phagocytosis is calcium independent, whereas Fc $\gamma$ RII-mediated phagocytosis requires a sustained rise in intracellular calcium. Fc $\gamma$ RI and Fc $\gamma$ RIIa aggregation stimulate the MEK1/ERK pathway, but Fc $\gamma$ RI activates this pathway to a greater extent.

When we compared secreted cytokines and chemokines induced by FcR cross-linking, Fc $\gamma$ RI activation elicits the production of higher levels of the proinflammatory mediators TNF- $\alpha$ , IL-8, IL-6, IFN- $\gamma$ , G-CSF, and MIP-1 $\beta$ . This suggests that Fc $\gamma$ RI may play a dominant role over Fc $\gamma$ RIIa in the augmentation of inflammation and immunity. This conclusion is supported by data on membrane trafficking and antigen presentation. Immune complexes internalized via Fc $\gamma$ RI traffic to membrane-processing compartments termed MIICs, in which antigens are broken down into short peptides for loading onto MHC class II molecules.<sup>47</sup> When we induce the internalization of Fc $\gamma$ RI or Fc $\gamma$ RIIa in U937, we observe some overlap in staining between Fc $\gamma$ RI and Fc $\gamma$ RIIa, particularly in the early endocytic markers EEA-1, TI-VAMP, and syntaxin 4. However, over an identical period, Fc $\gamma$ RIIa traffics to compartments that are negative for HLA-DM or LAMP-1, suggesting that they do not traffic to MIICs.

The extension of these observations to primary monocytes and dendritic cells is complicated by the presence of an additional Fc $\gamma$ R. Fc $\gamma$ RIIb is an immune-tyrosine inhibitory motif-containing inhibitory Fc $\gamma$ R that regulates the signaling activity of other activatory FcRs. It has been shown that Fc $\gamma$ RIIb expression in primary monocytes taken from healthy individuals is restricted to a small subset of cells.<sup>48</sup> Our studies have shown that the signaling and membrane-trafficking events observed in U937 also apply to primary human

monocytes, suggesting that the signaling pathways described here remain applicable to primary cells despite the possible coexpression of Fc $\gamma$ RIIb on a small subset. In primary monocytes, complexes internalized via Fc $\gamma$ RI localize to MIICs, whereas those internalized via Fc $\gamma$ RIIa do not. This results in a marked difference in the ability of the monocytes to present antigens, derived from the immune complexes to influenza-A-specific CD4<sup>+</sup> T lymphocytes. Fc $\gamma$ RI exhibits significant dominance over Fc $\gamma$ RIIa in the presentation of internalized antigens.

An additional complicating factor in our interpretation of the signaling activity of Fc $\gamma$ RI is the possibility that mouse antibodies used to cross-link Fc $\gamma$ RI coengage Fc $\gamma$ RIIa on the surface of the cells. Based on our current antibody cross-linking methodologies, it is impossible to rule this out. However, it is also clear from our studies on immune-complex-mediated stimulation of primary human monocytes in which Fc $\gamma$ RIIa is blocked with IV.3 that Fc $\gamma$ RI signaling overlaps with our observations on antibody cross-linking, suggesting that coengagement of Fc $\gamma$ RIIa is not a significant factor.

The physiologic significance of the distinct signaling pathways and antigenic fates subserved by Fc $\gamma$ RI and Fc $\gamma$ RIIa remains to be determined. Although the 2 receptors are often expressed on the same cell type, their ratios differ on different cells and may be further altered by differential regulation by cytokines, etc, in diverse immunologic contexts. Differential signaling between the two could also be influenced by the affinities of each receptor for distinct IgG isotypes, which are known to vary widely between immune responses (eg, T-dependent versus T-independent, or T<sub>H</sub>1 vs T<sub>H</sub>2). For example, only Fc $\gamma$ RIIa binds IgG2, and autoimmunity associated polymorphisms in Fc $\gamma$ RIIa alter isotype affinity and have significant functional implications.<sup>49</sup>

Finally, the effect of the inhibitory Fc $\gamma$ RIIb, itself tightly regulated, might favor signaling through Fc $\gamma$ RI or Fc $\gamma$ RIIa in different circumstances. Thus, summation of effects of the different IgG isotypes produced during immune responses, along with the regulation of FcRs on the different cell types, could harness the distinct signaling pathways we have described for Fc $\gamma$ RI and Fc $\gamma$ RIIa to control antigenic fate and immune outcome in health and disease.

Taken together, these data suggest fundamental differences in the activities of the 2 FcRs, with important implications for inflammation and immune homeostasis. Fc $\gamma$ RI uptake and signaling primes human immune cells to enhance inflammation and antigen presentation, whereas Fc $\gamma$ RIIa does not. New therapeutic strategies aimed at inducing an absolute switch in the activation of signaling pathways triggered by Fc $\gamma$ RI or Fc $\gamma$ RIIa may also provide the means to control the nature of potentially harmful or protective immune responses in infection and autoimmunity.

## Supplementary Material

Refer to Web version on PubMed Central for supplementary material.

## Acknowledgments

We thank Dr. Adrian Kelly (Cambridge University, United Kingdom) for providing the rabbit anti-HLA-DM used in this study. We also thank A.-K. Fraser-Andrews for proofreading the manuscript.

This work was supported by a Singapore-MIT Alliance for Research and Technology (SMART-MIT) Pilot project grant and Biomedical Research Council (BMRC) and Office of Life Sciences (OLS)–Young Investigator awards.

## References

- Hogarth PM. Fc receptors are major mediators of antibody based inflammation in autoimmunity. *Curr Opin Immunol.* 2002; 14:798–802. [PubMed: 12413532]
- Hulett MD, Hogarth PM. Molecular basis of Fc receptor function. *Adv Immunol.* 1994; 57:1–127. [PubMed: 7872156]
- Ravetch JV, Kinet JP. Fc receptors. *Annu Rev Immunol.* 1991; 9:457–492. [PubMed: 1910686]
- Allen JM, Seed B. Isolation and expression of functional high-affinity Fc receptor complementary DNAs. *Science.* 1989; 243:378–381. [PubMed: 2911749]
- Graziano RF, Fanger MW. Fc gamma RI and Fc gamma RII on monocytes and granulocytes are cytotoxic trigger molecules for tumor cells. *J Immunol.* 1987; 139:3536–3541. [PubMed: 2960735]
- van de Winkel JG, Capel PJ. Human IgG Fc receptor heterogeneity: molecular aspects and clinical implications. *Immunol Today.* 1993; 14:215–221. [PubMed: 8517920]
- Sanchez-Mejorada G, Rosales C. Signal transduction by immunoglobulin Fc receptors. *J Leukoc Biol.* 1998; 63:521–533. [PubMed: 9581795]
- Melendez A, Floto RA, Cameron AJ, Gillooly DJ, Harnett MM, Allen JM. A molecular switch changes the signalling pathway used by the Fc gamma RI antibody receptor to mobilise calcium. *Curr Biol.* 1998; 8:210–221. [PubMed: 9501983]
- Reefman E, Dijstelbloem HM, Limburg PC, Kallenberg CG, Bijl M. Fc gamma receptors in the initiation and progression of systemic lupus erythematosus. *Immunol Cell Biol.* 2003; 81:382–389. [PubMed: 12969326]
- Melendez AJ, Gillooly DJ, Harnett MM, Allen JM. Aggregation of the human high affinity immunoglobulin G receptor (Fc gamma RI) activates both tyrosine kinase and G protein-coupled phospho-inositide 3-kinase isoforms. *Proc Natl Acad Sci U S A.* 1998; 95:2169–2174. [PubMed: 9482857]
- Ely P, Wallace PK, Givan AL, Graziano RF, Guyre PM, Fanger MW. Bispecific-armed, interferon gamma-primed macrophage-mediated phagocytosis of malignant non-Hodgkin's lymphoma. *Blood.* 1996; 87:3813–3821. [PubMed: 8611707]
- Huang ZY, Hunter S, Kim MK, et al. The monocyte Fc gamma receptors Fc gamma RI/gamma and Fc gamma RIIA differ in their interaction with Syk and with Src-related tyrosine kinases. *J Leukoc Biol.* 2004; 76:491–499. [PubMed: 15136586]
- Clatworthy MR, Smith KG. Fc gamma RIIB balances efficient pathogen clearance and the cytokine-mediated consequences of sepsis. *J Exp Med.* 2004; 199:717–723. [PubMed: 14981111]
- Wang WK, Chen HL, Yang CF, et al. Slower rates of clearance of viral load and virus-containing immune complexes in patients with dengue hemorrhagic fever. *Clin Infect Dis.* 2006; 43:1023–1030. [PubMed: 16983615]
- Van de Winkel JG, Tax WJM, Jacobs CWM, Huizinga TWJ, Willems PHGM. Cross-linking of both types of IgG Fc receptors, Fc gamma RI and Fc gamma RII, enhances intracellular free Ca<sup>2+</sup> in the monocytic cell line U937. *Scand J Immunol.* 1990; 31:315–325. [PubMed: 2157275]
- Melendez A, Floto RA, Gillooly DJ, Harnett MM, Allen JM. Fc gamma RI coupling to phospholipase D initiates sphingosine kinase-mediated calcium mobilization and vesicular trafficking. *J Biol Chem.* 1998; 273:9393–9402. [PubMed: 9545263]
- Melendez AJ, Harnett MM, Allen JM. Fc gamma RI activation of phospholipase C gamma 1 and protein kinase C in dibutyryl cAMP-differentiated U937 cells is dependent solely on the tyrosine-kinase activated form of phosphatidylinositol-3-kinase. *Immunology.* 1999; 98:1–8. [PubMed: 10469227]

18. Melendez AJ, Harnett MM, Allen JM. Differentiation-dependent switch in protein kinase C isoenzyme activation by FcγRI, the human high-affinity receptor for immunoglobulin G. *Immunology*. 1999; 96:457–464. [PubMed: 10233728]
19. Tay HK, Melendez AJ. FcγRI-triggered generation of arachidonic acid and eicosanoids requires iPLA2 but not cPLA2 in human monocytic cells. *J Biol Chem*. 2004; 279:22505–22513. [PubMed: 15007079]
20. Beekman JM, van der Linden JA, van de Winkel JG, Leusen JH. FcγRI (CD64) resides constitutively in lipid rafts. *Immunol Lett*. 2008; 116:149–155. [PubMed: 18207250]
21. Barnes N, Gavin AL, Tan PS, Mottram P, Koentgen F, Hogarth PM. FcγRI-deficient mice show multiple alterations to inflammatory and immune responses. *Immunity*. 2002; 16:379–389. [PubMed: 11911823]
22. Kwiatkowska K, Frey J, Sobota A. Phosphorylation of FcγRIIA is required for the receptor-induced actin rearrangement and capping: the role of membrane rafts. *J Cell Sci*. 2003; 116:537–550. [PubMed: 12508114]
23. Larrick JW, Fischer DG, Anderson SJ, Koren HS. Characterization of a human macrophage-like cell line stimulated in vitro: a model of macrophage functions. *J Immunol*. 1980; 125:6–12. [PubMed: 7381211]
24. Lubeck MD, Steplewski Z, Baglia F, Klein MH, Dorrington KJ, Koprowski H. The interaction of murine IgG subclass proteins with human monocyte Fc receptors. *J Immunol*. 1985; 135:1299–1304. [PubMed: 3159790]
25. Melendez AJ, Bruetsch L, Floto RA, Harnett MM, Allen JM. Functional coupling of FcγRI to nicotinamide adenine dinucleotide phosphate (reduced form) oxidative burst and immune complex trafficking requires the activation of phospholipase D1. *Blood*. 2001; 98:3421–3428. [PubMed: 11719383]
26. Melendez AJ, Harnett MM, Allen JM. Crosstalk between ARF6 and protein kinase Calpha in Fc(γ)RI-mediated activation of phospholipase D1. *Curr Biol*. 2001; 11:869–874. [PubMed: 11516649]
27. Melendez AJ, Harnett MM, Pushparaj PN, et al. Inhibition of Fc εRI-mediated mast cell responses by ES-62, a product of parasitic filarial nematodes. *Nat Med*. 2007; 13:1375–1381. [PubMed: 17952092]
28. Melendez AJ, Khaw AK. Dichotomy of Ca<sup>2+</sup> signals triggered by different phospholipid pathways in antigen stimulation of human mast cells. *J Biol Chem*. 2002; 277:17255–17262. [PubMed: 11856736]
29. Melendez AJ, Ibrahim FB. Antisense knockdown of sphingosine kinase 1 in human macrophages inhibits C5a receptor-dependent signal transduction, Ca<sup>2+</sup> signals, enzyme release, cytokine production, and chemotaxis. *J Immunol*. 2004; 173:1596–1603. [PubMed: 15265887]
30. Jayapal M, Tay HK, Reghunathan R, et al. Genome-wide gene expression profiling of human mast cells stimulated by IgE or FcεRI aggregation reveals a complex network of genes involved in inflammatory responses. *BMC Genomics*. 2006; 7:210. [PubMed: 16911805]
31. Reghunathan R, Jayapal M, Hsu LY, et al. Expression profile of immune response genes in patients with severe acute respiratory syndrome. *BMC Immunol*. 2005; 6:2. [PubMed: 15655079]
32. Bredius RG, de Vries CE, Troelstra A, et al. Phagocytosis of *Staphylococcus aureus* and *Haemophilus influenzae* type B opsonized with polyclonal human IgG1 and IgG2 antibodies: functional hFc γRIIa polymorphism to IgG2. *J Immunol*. 1993; 151:1463–1472. [PubMed: 8335940]
33. Issekutz T, Chu E, Geha RS. Antigen presentation by human B cells: T cell proliferation induced by Epstein Barr virus B lymphoblastoid cells. *J Immunol*. 1982; 129:1446–1450. [PubMed: 6286767]
34. Boni C, Fiscaro P, Valdatta C, et al. Characterization of hepatitis B virus (HBV)-specific T-cell dysfunction in chronic HBV infection. *J Virol*. 2007; 81:4215–4225. [PubMed: 17287266]
35. Floto RA, Clatworthy MR, Heilbronn KR, et al. Loss of function of a lupus-associated FcγRIIb polymorphism through exclusion from lipid rafts. *Nat Med*. 2005; 11:1056–1058. [PubMed: 16170323]

36. Tapper H. The secretion of preformed granules by macrophages and neutrophils. *J Leukoc Biol.* 1996; 59:613–622. [PubMed: 8656045]
37. Cathcart MK. Regulation of superoxide anion production by NADPH oxidase in monocytes/macrophages: contributions to atherosclerosis. *Arterioscler Thromb Vasc Biol.* 2004; 24:23–28. [PubMed: 14525794]
38. Trowsdale J, Hanson I, Mockridge I, Beck S, Townsend A, Kelly A. Sequences encoded in the class II region of the MHC related to the “ABC” superfamily of transporters. *Nature.* 1990; 348:741–744. [PubMed: 2259383]
39. Sanderson F, Kleijmeer MJ, Kelly A, et al. Accumulation of HLA-DM, a regulator of antigen presentation, in MHC class II compartments. *Science.* 1994; 266:1566–1569. [PubMed: 7985027]
40. Swain SL, Agrewala JN, Brown DM, et al. CD4+ T-cell memory: generation and multi-faceted roles for CD4+ T cells in protective immunity to influenza. *Immunol Rev.* 2006; 211:8–22. [PubMed: 16824113]
41. Watanabe Y, Hashimoto Y, Shiratsuchi A, Takizawa T, Nakanishi Y. Augmentation of fatality of influenza in mice by inhibition of phagocytosis. *Biochem Biophys Res Commun.* 2005; 337:881–886. [PubMed: 16216222]
42. Lakadamyali M, Rust MJ, Babcock HP, Zhuang X. Visualizing infection of individual influenza viruses. *Proc Natl Acad Sci U S A.* 2003; 100:9280–9285. [PubMed: 12883000]
43. Allen LA, Allgood JA. Atypical protein kinase C-zeta is essential for delayed phagocytosis of *Helicobacter pylori*. *Curr Biol.* 2002; 12:1762–1766. [PubMed: 12401171]
44. Allen LH, Aderem A. A role for MARCKS, the alpha isozyme of protein kinase C and myosin I in zymosan phagocytosis by macrophages. *J Exp Med.* 1995; 182:829–840. [PubMed: 7650489]
45. Larsen EC, DiGennaro JA, Saito N, et al. Differential requirement for classic and novel PKC isoforms in respiratory burst and phagocytosis in RAW 264.7 cells. *J Immunol.* 2000; 165:2809–2817. [PubMed: 10946313]
46. Zheng L, Zomerdijk TP, Aarnoudse C, van Furth R, Nibbering PH. Role of protein kinase C isozymes in Fc gamma receptor-mediated intracellular killing of *Staphylococcus aureus* by human monocytes. *J Immunol.* 1995; 155:776–784. [PubMed: 7608554]
47. Rocha N, Neefjes J. MHC class II molecules on the move for successful antigen presentation. *EMBO J.* 2008; 27:1–5. [PubMed: 18046453]
48. Veri MC, Gorlatov S, Li H, et al. Monoclonal antibodies capable of discriminating the human inhibitory Fc gamma-receptor IIB (CD32B) from the activating Fc gamma-receptor IIA (CD32A): biochemical, biological and functional characterization. *Immunology.* 2007; 121:392–404. [PubMed: 17386079]
49. Salmon JE, Edberg JC, Brogle NL, Kimberly RP. Allelic polymorphisms of human Fc gamma receptor IIA and Fc gamma receptor IIIB: independent mechanisms for differences in human phagocyte function. *J Clin Invest.* 1992; 89:1274–1281. [PubMed: 1532589]

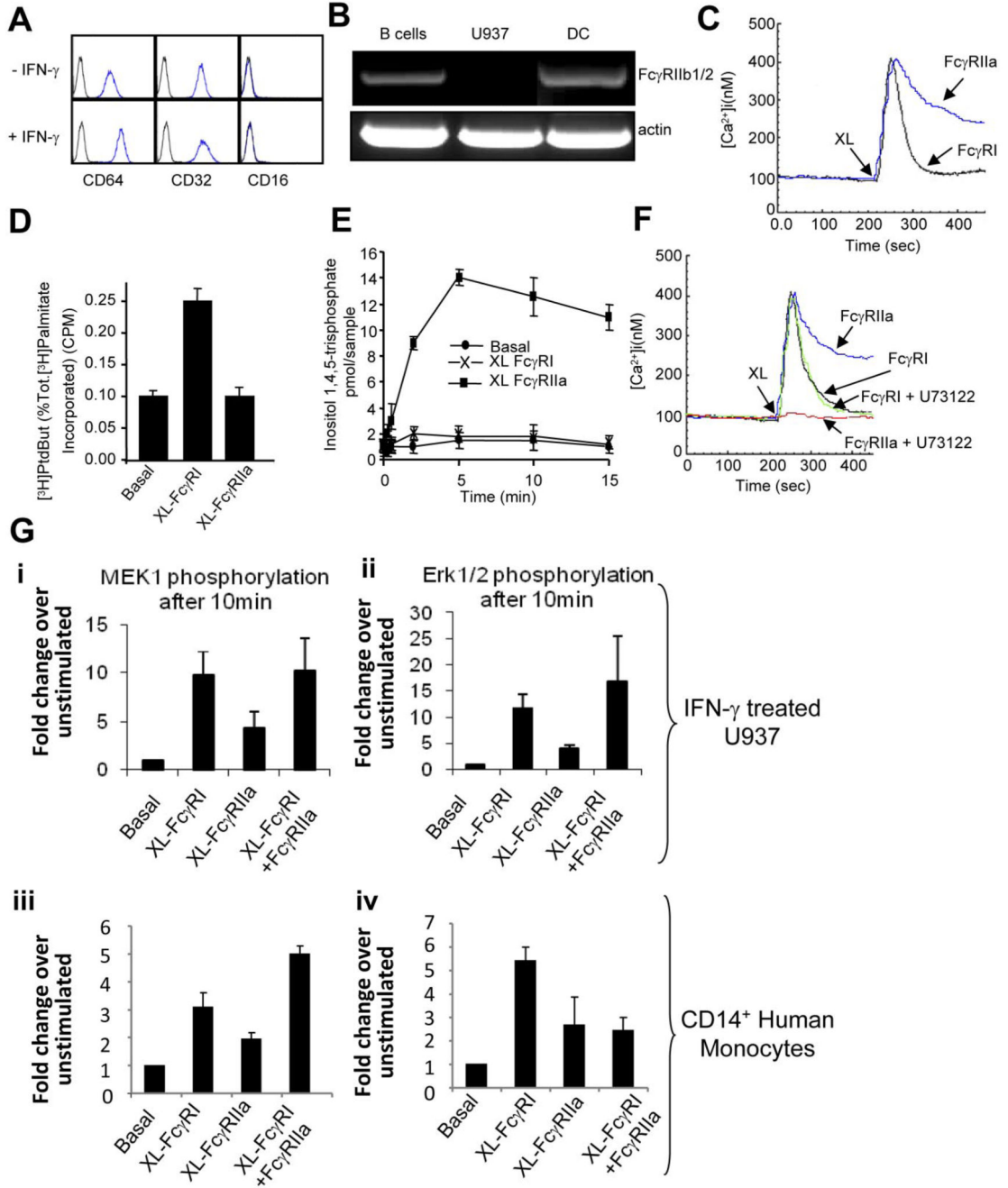


**Figure 1. FcR expression and signaling in U937 and primary monocytes.**  
 (A) U937 cells express Fc $\gamma$ RI and Fc $\gamma$ RII, but not Fc $\gamma$ RIII, as determined by flow cytometry using anti-CD32PE and anti-CD64PE and anti-CD16PE (BD Pharmingen). (B) RT-PCR was used to assess the expression of Fc $\gamma$ RIIb1/2 on U937 compared with B lymphocytes and dendritic cells. (C) Fc $\gamma$ RI and Fc $\gamma$ RIIa trigger differential cytosolic Ca<sup>2+</sup> signals. Cytosolic calcium was measured in U937 by cuvette fluorimetry over 8 minutes after cross-linking of the individual FcRs using antibody clones 10.1 and 3D3 (BD Pharmingen), respectively (XL). (D) Fc $\gamma$ RI triggers PLD activity, whereas Fc $\gamma$ RIIa does

not. PLD activity measured in resting U937 cells (Basal) or in cells after Fc $\gamma$ R aggregation (XL Fc $\gamma$ RI or XL Fc $\gamma$ RIIa) for 30 minutes. (E) Fc $\gamma$ RIIa triggers PLC activation in U937 cells. InsP<sub>3</sub> generation was measured in resting cells (basal) or in cells after Fc $\gamma$ R aggregation (XL Fc $\gamma$ RI or XL Fc $\gamma$ RIIa) for 15 minutes. (F) The PLC inhibitor U73122 blocks the Fc $\gamma$ RIIa-mediated cytosolic calcium signal in U937 cells. Cells pretreated with the PLC inhibitor U73122 for 45 minutes were assayed for cytosolic calcium over 8 minutes after FcR cross-linking (XL Fc $\gamma$ RI or XL Fc $\gamma$ RIIa). (G) In IFN- $\gamma$ -treated U937 (i-ii) and primary human monocytes (iii-iv), MEK1 and ERK1/2 are activated by Fc $\gamma$ RI ligation by antibody clone 10.1 to a greater extent than by Fc $\gamma$ RIIa ligation by antibody clone 3D3. Phosphoprotein array (Biorad) was used to measure ERK1/2 and MEK1 phosphorylation in cell lysates. MEK1, ERK, PLC, and PLD activity is expressed as a mean  $\pm$  SD from 3 independent experiments. All intracellular calcium measurements were carried out in the presence of 1.5 M extracellular calcium and results shown are typical of 3 independent experiments.

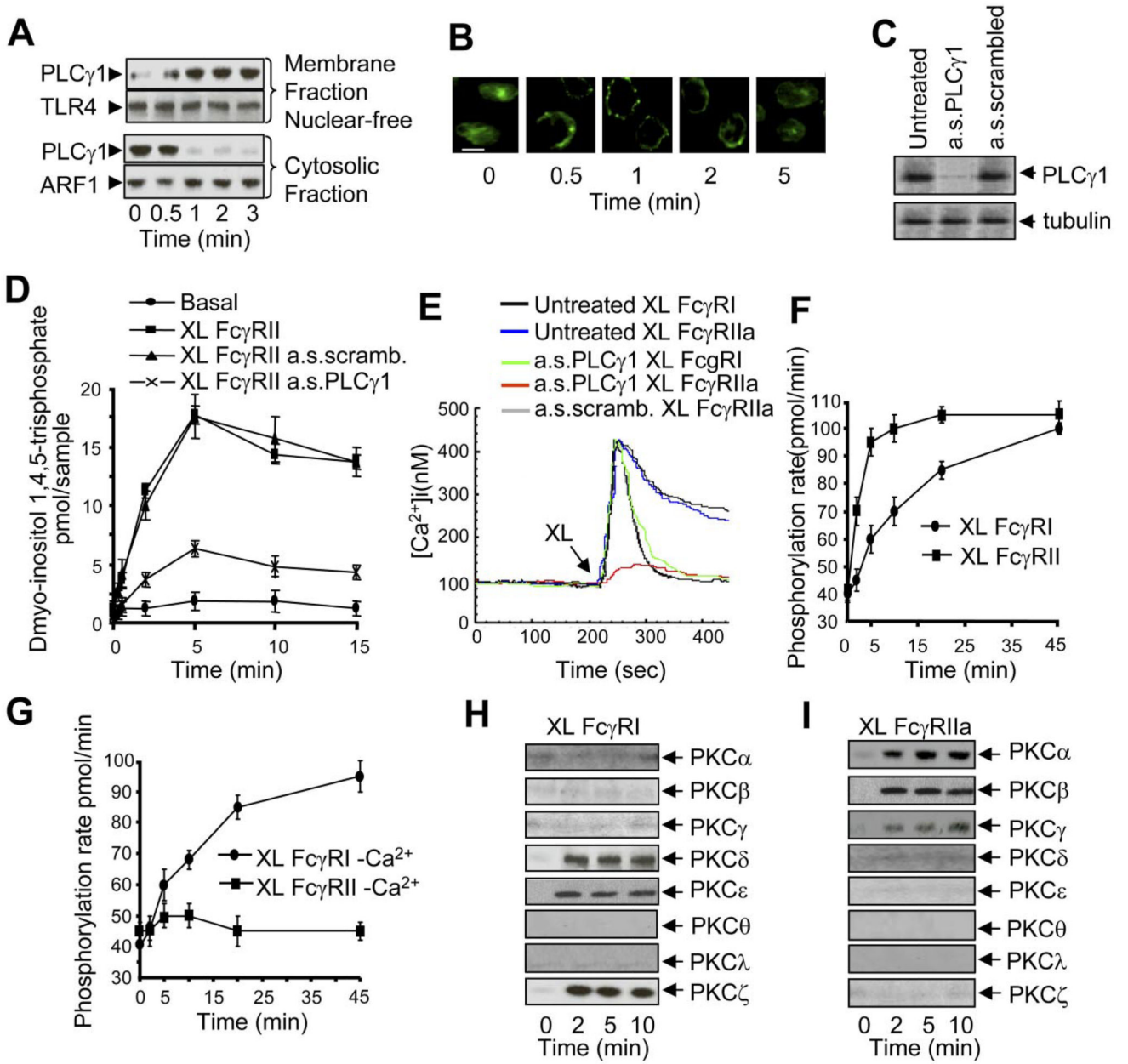


**Figure 2. Fc $\gamma$ RIIa triggers PLC $\gamma$ 1 activity, PLC $\gamma$ 1 dependent Ca<sup>2+</sup> signals, and PKC activity in U937.**

(A) Immunoblot analysis was used to assay PLC $\gamma$ 1 translocation after Fc $\gamma$ RIIa activation by antibody cross-linking in U937. A comparison is shown between a nuclear-free membrane-fraction (top panels) with the cytosolic fraction (bottom panels) probed with an anti-PLC $\gamma$ 1 antibody. TLR-4 and ARF were analyzed as loading controls for the membrane fraction and cytosolic fractions, respectively. (B) U937 stained for PLC $\gamma$ 1 after Fc $\gamma$ RIIa cross-linking using antibody clone 3D3 over 5 minutes. Scale bar indicates 20  $\mu$ m. (C) U937 pretreated with anti-PLC $\gamma$ 1 oligonucleotides down-regulate PLC $\gamma$ 1. Immunoblot analysis of untreated cells, treated cells (a.s.PLC $\gamma$ 1), and scrambled oligo (a.s.scrambled) as a control.  $\alpha$ -Tubulin

was used as a loading control. (D) Fc $\gamma$ RIIa signals through PLC $\gamma$ 1. InsP<sub>3</sub> generation was used as a readout for PLC $\gamma$ 1 activation. Basal controls compared with Fc $\gamma$ RIIa activation (XL Fc $\gamma$ RIIa) and with cells pretreated with antisense oligo (XL Fc $\gamma$ RIIa a.s.PLC $\gamma$ 1) or scrambled oligo (XL Fc $\gamma$ RIIa a.s.scramb.). (E) PLC $\gamma$ 1 activation by Fc $\gamma$ RIIa is linked to cytosolic calcium signaling in U937. Cytosolic calcium signals in U937 were assayed by cuvette fluorimetry after FcR aggregation (untreated XL Fc $\gamma$ RI or untreated XL Fc $\gamma$ RIIa) compared with cells pretreated with antisense oligo against PLC $\gamma$ 1 (a.s.PLC $\gamma$ 1 XL Fc $\gamma$ RI or a.s.PLC $\gamma$ 1 XL Fc $\gamma$ RIIa) or a scrambled oligo control (a.s.scramb. XL Fc $\gamma$ RIIa). (F) PKC activity in the presence of Ca<sup>2+</sup> was measured as the phosphorylation rate (pmol/min) in samples from whole cell lysates after aggregation of Fc $\gamma$ RI (labeled XL Fc $\gamma$ RI) or Fc $\gamma$ RIIa (XL Fc $\gamma$ RIIa). (G) PKC activity in the absence of Ca<sup>2+</sup> was similarly measured. (H) Fc $\gamma$ RI-mediated PKC isoform translocation. Immunoblot analysis of different PKC isoenzymes translocated to the nuclear-free membrane fraction after antibody-mediated Fc $\gamma$ RI aggregation over 10 minutes. (I) Fc $\gamma$ RIIa-mediated PKC isoform translocation similarly measured in nuclear-free membrane fractions. Immunoblots and calcium traces shown are typical from at least 3 separate experiments. Graphic data represent mean  $\pm$  SD from 3 experiments.

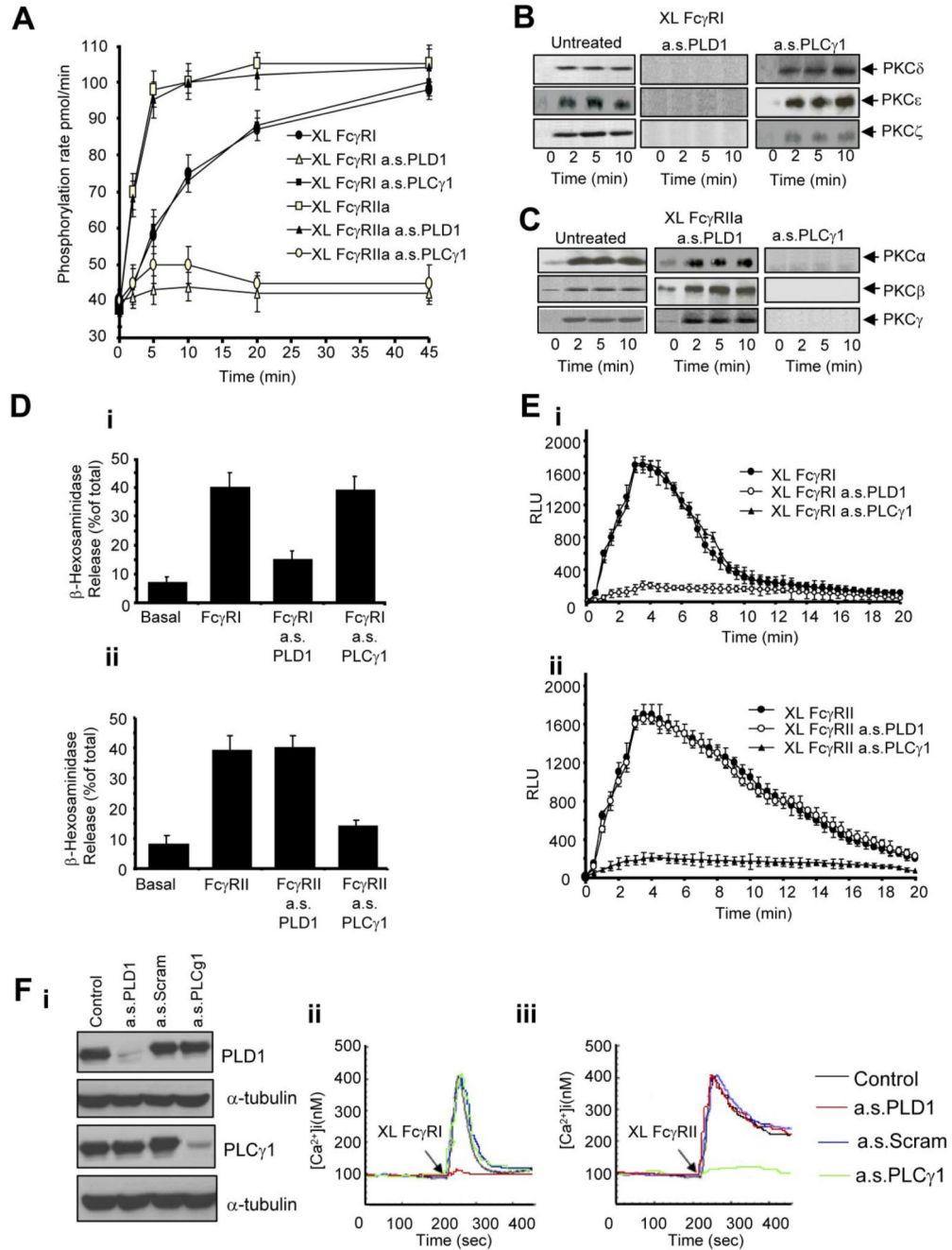


**Figure 3. Role of PLD1 and PLC $\gamma$ 1 in Fc $\gamma$ RI- and Fc $\gamma$ RIIa-mediated signaling.**

(A) Fc $\gamma$ RI- and Fc $\gamma$ RIIa-mediated PKC activity measured as the phosphorylation rate (pmol/min) in whole-cell lysates. Antibody-mediated Fc $\gamma$ R aggregation in untreated cells (XL Fc $\gamma$ RI (antibody 10.1) or XL Fc $\gamma$ RIIa (antibody 3D3), cells pretreated with the antisense oligos against PLD1 (XL Fc $\gamma$ RI a.s.PLD1 or XL Fc $\gamma$ RIIa a.s.PLD1), or antisense oligos against PLC $\gamma$ 1 (XL Fc $\gamma$ RI a.s.PLC $\gamma$ 1 or XL Fc $\gamma$ RIIa a.s.PLC $\gamma$ 1). (B) Fc $\gamma$ RI-mediated PKC isoform translocation requires PLD1. Immunoblot analysis of the PKC isoenzymes translocated to the nuclear-free membrane fraction after antibody-mediated

Fc $\gamma$ RI aggregation in control cells (untreated) and cells pretreated with the antisense oligos against PLD1 or PLC $\gamma$ 1 (a.s.PLD1 or a.s.PLC $\gamma$ 1). (C) Fc $\gamma$ RIIa-mediated PKC isoform translocation requires PLC $\gamma$ 1. The same analyses applied to cells after Fc $\gamma$ RIIa activation. (D) Fc $\gamma$ RI and Fc $\gamma$ RIIa-mediated degranulation. (i)  $\beta$ -Hexosaminidase release in resting cells (basal) or after antibody-mediated Fc $\gamma$ RI aggregation in control cells (XL Fc $\gamma$ RI) compared with cells pretreated with antisense oligonucleotides to either PLD1 (XL Fc $\gamma$ RI a.s.PLD1) or PLC $\gamma$ 1 (XL Fc $\gamma$ RI a.s.PLC $\gamma$ 1). (ii) The same analyses applied to cells after Fc $\gamma$ RIIa activation. (E) Fc $\gamma$ RI and Fc $\gamma$ RIIa-mediated activation of NADPH oxidative burst. (i) Superoxide production in response to antibody-mediated Fc $\gamma$ RI activation in control cells (XL Fc $\gamma$ RI) compared with cells pretreated with antisense oligos to either PLD1 (XL Fc $\gamma$ RI a.s.PLD1) or PLC $\gamma$ 1 (XL Fc $\gamma$ RI a.s.PLC $\gamma$ 1). (ii) The same analyses applied to cells after Fc $\gamma$ RIIa activation. Results expressed are the mean  $\pm$  SD of triplicate samples of 3 independent experiments. (Fi) Primary human monocytes pretreated with anti-PLD1 or anti-PLC $\gamma$ 1 oligonucleotides down-regulate PLD1 and PLC $\gamma$ 1, respectively, compared with  $\alpha$ -tubulin controls. (Fii) Monocytes treated with anti-PLD1 oligonucleotides are impaired in their cytosolic calcium signaling after activation of Fc $\gamma$ RI by receptor crosslinking using antibody clone 10.1. (Fiii) Monocytes treated with anti-PLC $\gamma$ 1 oligonucleotides are impaired in their cytosolic calcium signaling after activation of Fc $\gamma$ RIIa by receptor crosslinking using antibody clone 3D3.

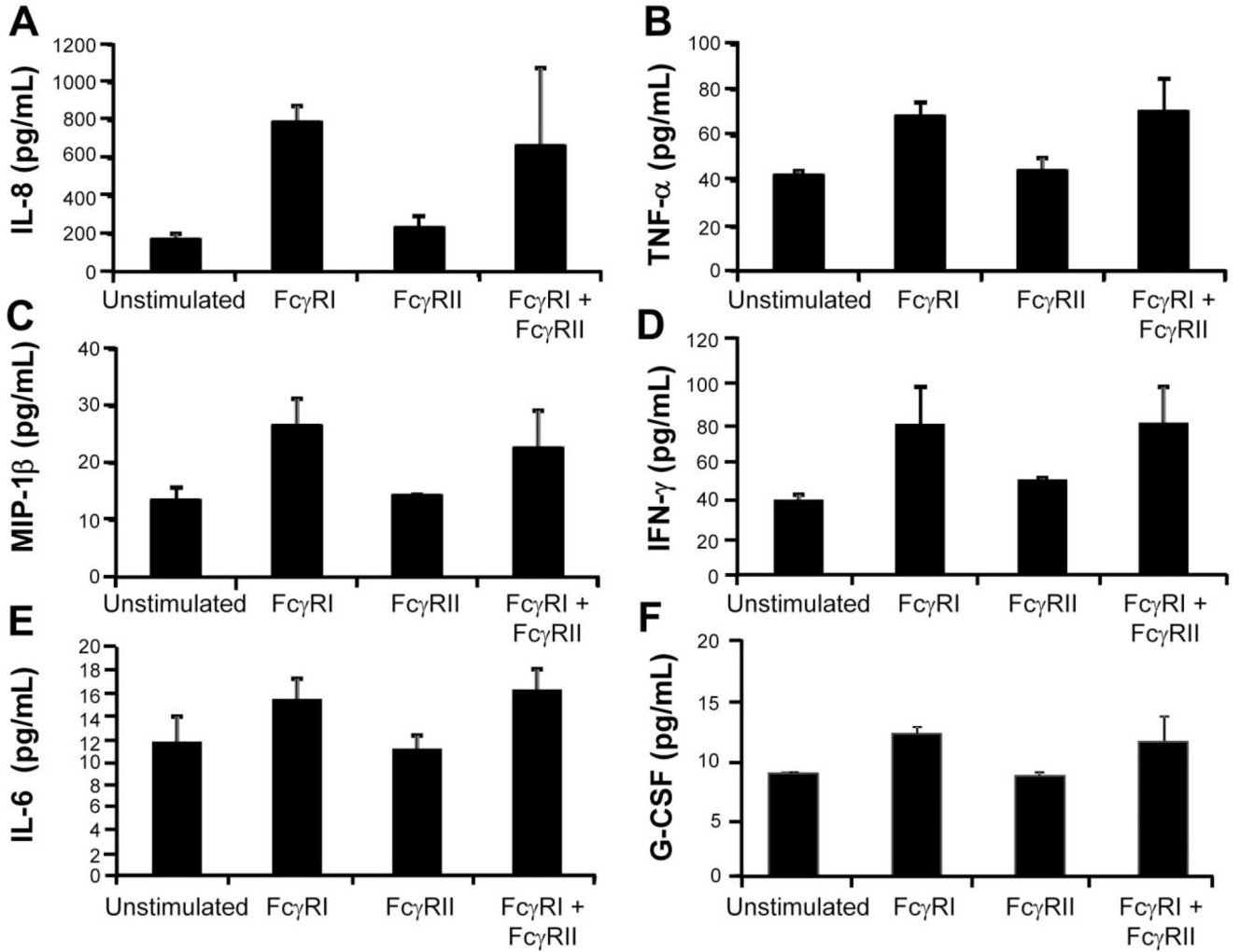


**Figure 4. Differential cytokine/chemokine release triggered by Fc $\gamma$ RI versus Fc $\gamma$ RIIa activation.** U937 cells were cross-linked with anti-CD32 (antibody 3D3) and/or anti-CD64 (antibody 10.1) plus goat anti-mouse IgG F(ab) $'_2$  for 10 minutes and cells were placed in culture for 24 hours. Culture supernatants were harvested 24 hours later and assayed for 17 different cytokine targets by Bioplex cytokine array analysis. Higher levels of (A) IL-8, (B) TNF- $\alpha$ , (C) MIP-1 $\beta$ , (D) IFN- $\gamma$ , (E) IL-6, and (F) G-CSF were secreted after cross-linking of Fc $\gamma$ RI versus Fc $\gamma$ RIIa. Results are expressed as the mean  $\pm$  SD of triplicate samples from 4 independent experiments.

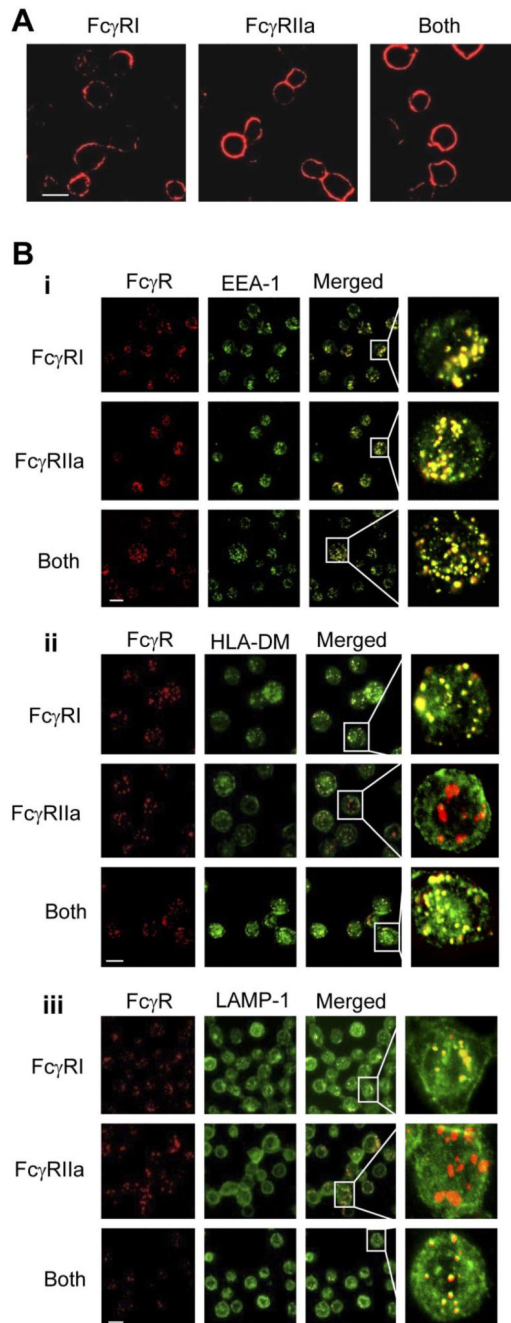


**Figure 5. Differential membrane trafficking of Fc $\gamma$ RI and Fc $\gamma$ RIIa receptors.**

Fc $\gamma$ RI or Fc $\gamma$ RII were cross-linked with mouse anti-human CD64 (antibody 10.1) and/or mouse anti-human CD32 (antibody 3D3), respectively. The secondary monoclonal used for cross-linking the specific mAbs in these experiments was an Alexa Fluor 647–conjugated goat anti–mouse IgG F(ab) $'_2$  (Invitrogen). Receptors were cross-linked for 10 minutes at 37°C to allow internalization. At this time point, cells were fixed and frozen in methanol/acetone (1:1) at –20°C for at least 24 hours before further staining. (A) In the absence of FcR cross-linking, Fc $\gamma$ RI and Fc $\gamma$ RIIa remain localized at the cell surface. (B) After FcR

cross-linking for 10 minutes, (i) both receptors enter a compartment that stains positive for the early endosome marker EEA-1. However, whereas Fc $\gamma$ RI enters a compartment that also stains positive for (ii) HLA-DM and (iii) LAMP-1, Fc $\gamma$ RIIa enters a compartment that is negative for both these markers of MIIC compartments. Scale bar indicates 20  $\mu$ m. Results shown are typical of at least 3 separate experiments. Anti-EEA-1 and anti-LAMP1 polyclonal antibodies were purchased from Santa Cruz. Rabbit anti-HLA-DM was provided by Dr Adrian Kelly (Immunology Unit, Department of Pathology, Cambridge University, Cambridge, United Kingdom).

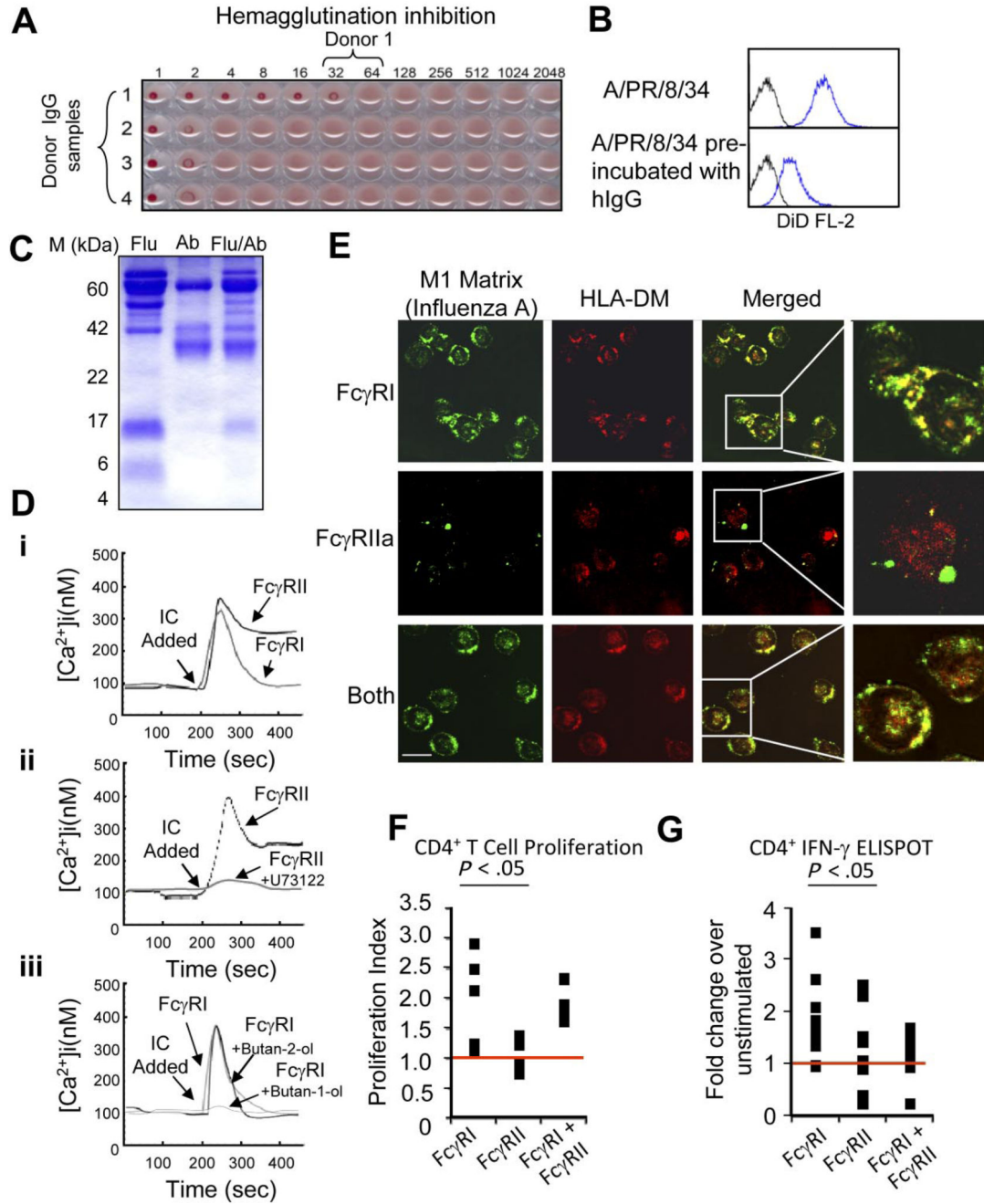


**Figure 6. Antigen/immune complexes internalized through FcγRI are presented more efficiently to CD4<sup>+</sup> T cells.**

(A) A hemagglutination inhibition assay was used on serum samples from a panel of influenza A–vaccinated human donors to identify samples contained high levels of anti–influenza A (strain A/PR/8/34) hlgG. (B) Flow cytometric analysis of live influenza A virus labeled with the lipophilic fluorescent dye 1,1′-dioctadecyl-3,3,3′,3′-tetramethylindodicarbocyanine binding to U937 cells (top histogram); 1 μM of hlgG isolated from donor 1 inhibits the binding of the live virus (bottom histogram). (C) Purified immune complexes (IC) generated by incubating live influenza A virus with hlgG from donor 1

(Flu/Ab) exhibit protein bands from both the virus (Flu) and hIgG (Ab). (Di) Cytosolic calcium signaling in primary human monocytes stimulated with IC. IC-mediated Fc $\gamma$ RI Ca<sup>2+</sup> signaling was analyzed in the presence of a blocking antibody to Fc $\gamma$ RII, IV.3. Fc $\gamma$ RIIa signaling was analyzed in presence of excess hIgG to ensure receptor occupancy and blockade of Fc $\gamma$ RI. (Dii) IC-mediated Fc $\gamma$ RIIa induced cytosolic Ca<sup>2+</sup> in primary monocytes treated with the PLC- $\gamma$  inhibitor U73122 versus untreated controls. (Diii) IC-mediated Fc $\gamma$ RI induced cytosolic Ca<sup>2+</sup> in primary monocytes treated with the PLD inhibitor butan-1-ol (0.3%) versus butan-2-ol (0.3%) and untreated controls. (E) Top panel: Fc $\gamma$ RIIa is blocked with antibody IV.3 to allow for Fc $\gamma$ RI-mediated internalization of IC into primary human monocytes into endocytic compartments that stain positive for HLA-DM, the putative MIIC marker, and the influenza A matrix protein (M1 matrix). Middle panel: Fc $\gamma$ RI is blocked with excess hIgG to allow for IC internalization via Fc $\gamma$ RIIa. Bottom panel: IC uptake via both Fc $\gamma$ RI and Fc $\gamma$ RIIa in the absence of receptor blockade. (F) Human monocytes that internalize influenza A/hIgG IC via Fc $\gamma$ RI versus Fc $\gamma$ RIIa stimulate greater proliferation in influenza-A-specific CD4<sup>+</sup> human T lymphocyte cell lines; 5 cell lines derived from 3 unrelated human donors were tested with syngeneic monocytes pulsed with IC for 10 minutes in the presence or absence of Fc $\gamma$ RI or Fc $\gamma$ RIIa-blocking antibodies. 3H-Thymidine incorporation was used to measure cell proliferation and the resulting data expressed as a proliferation index. (G) ELISPOT analyses of influenza-A-specific CD4T-cell responses in primary human cells. Monocytes and CD4<sup>+</sup> T cells were enriched by CD8 depletion before internalization of IC via Fc $\gamma$ RI and/or Fc $\gamma$ RIIa. More than 9 independent experiments were carried out on unrelated human donors, the numbers of resulting ELISPOTs were assayed from 14 to 18 hours poststimulation using a CTL ImmunoSpot S4 analyzer. The fold difference between the number of spots per treatment condition over controls was calculated. An ANOVA analysis, followed by a protected *t* test, was conducted between the different conditions used for the proliferation assay and the IFN- $\gamma$  ELISPOT, and the significance levels are as reported. All intracellular calcium measurements were carried out in the presence of 1.5 M extracellular Calcium and results shown are typical of 3 independent experiments.